ELSEVIER

Journal of Alloys and Compounds 329 (2001) 108–114

Journal of ALLOYS AND COMPOUNDS

www.elsevier.com/locate/jallcom

Titanium catalyzed solid-state transformations in $LiAlH_4$ during high-energy ball-milling

V.P. Balema[a], J.W. Wiench[a], K.W. Dennis[a], M. Pruski[a], V.K. Pecharsky[a,b,*]

[a]*Ames Laboratory, Iowa State University, Ames, IA 50011-3020, USA*
[b]*Department of Materials Science and Engineering, Iowa State University, Ames, IA 50011, USA*

Received 28 February 2001; received in revised form 7 May 2001; accepted 7 May 2001

Abstract

Mechanical processing of polycrystalline $LiAlH_4$ in the presence of titanium- and iron-based catalysts induces the transformation of $LiAlH_4$ into Li_3AlH_6, Al and H_2 at room temperature. Several catalysts were tested and it was established that their activity gradually decreases from $TiCl_4$ to Fe in the series $TiCl_4 > Al_3Ti \gg Al_{22}Fe_3Ti_8 > Al_3Fe > Fe$. The high catalytic activity of $TiCl_4$ has been attributed to microcrystalline intermetallic Al_3Ti, which rapidly forms in situ from $TiCl_4$ and $LiAlH_4$ during mechanical processing and then acts as a heterogeneous dehydrogenation catalyst.

Keywords: Lithium aluminum hydride; Mechanochemistry; Solid state catalysis

1. Introduction

High capacity solid-state storage of hydrogen at ambient conditions is expected to become increasingly important as fuel cell power plants approach broad use in automotive and electrical utility applications. Aluminum-based complex metal hydrides, such as sodium and lithium aluminohydrides ($NaAlH_4$ and $LiAlH_4$), attract considerable attention as potential ultra-high-capacity hydrogen storage media [1–9] because their hydrogen content reaches 7.4 to 10.5% of hydrogen by weight, respectively. Several fundamentally different approaches to the development of aluminohydride-based hydrogen storage technology were proposed during the last few years. The first group of methods, which was developed for a low-temperature (i.e. at ambient conditions) generation of hydrogen gas from complex alkali metal aluminohydrides, involves chemical decomposition of hydrides with appropriate chemical reagents such as water [10–13] or ammonia [11]. Although this approach enables extraction of the entire hydrogen content from alkali metal aluminohydrides, it is unsuitable for the development of a reversible hydrogen storage system as it results in complete chemical decomposition of aluminohydrides. The second approach is based on the reversible thermal decomposition of sodium aluminohydride ($NaAlH_4$) in the presence of transition metal catalysts [2–7]. It has been reported that Ti-, Zr- and Fe-based inorganic or organometallic catalysts lower the decomposition temperature of $NaAlH_4$ by approximately 80°C. The Zr and Ti catalysts also make hydrogen release from sodium aluminohydride partially reversible at acceptable conditions, i.e. absorption of hydrogen occurs at temperatures between 150 and 165°C, and hydrogen pressure between 100 and 200 atm [6]. However, since the nature of the transition metal intermediates catalyzing hydrogen release and uptake in the doped $NaAlH_4$ is unknown [2–7], there is no clear understanding of how further development of aluminohydride-based hydrogen storage materials could be carried out most effectively. Furthermore, because of the relatively low hydrogen content (5.6 wt.% H_2 when $NaAlH_4$ decomposes to NaH, Al and H_2), sodium aluminohydride appears to be inferior to other hydrides such as lithium aluminohydride (7.9 wt.% H_2 when decomposed to LiH, Al and H_2) and magnesium hydride (7.6 wt.% H_2).

Recently, we reported that lithium aluminohydride can be easily transformed into lithium hexahydroaluminate (Li_3AlH_6), aluminum and hydrogen in the presence of catalytic amounts of metallic iron or titanium tetrachloride ($TiCl_4$) during high-energy ball-milling at room temperature [8,9]. Here, we describe our most recent results on mechanochemical transformations in $LiAlH_4$ in the pres-

*Corresponding author. 242 Spedding, Ames Laboratory, Ames, IA 50011-3020, USA. Tel.: +1-515-294-8220; fax: +1-515-294-9579.
E-mail address: vitkp@ameslab.gov (V.K. Pecharsky).

0925-8388/01/$ – see front matter
PII: S0925-8388(01)01570-5

ence of Ti- and/or Fe-based catalysts. The experimental data presented below demonstrate that the high catalytic activity of $TiCl_4$ reported in Ref. [8] is associated with in situ formation of a microcrystalline intermetallic Al_3Ti phase from $TiCl_4$ and $LiAlH_4$ during ball-milling. Once formed, Al_3Ti acts as a heterogeneous dehydrogenation catalyst.

2. Experimental

$LiAlH_4$ (≥98 wt.% pure) and $TiCl_4$ (99.995 wt.% pure) were purchased from Sigma–Aldrich. TiH_2 (99 wt.% pure) was purchased from Alfa. The intermetallic compounds were prepared from titanium, iron and aluminum (all were 99.999 wt.% pure), purchased from various commercial vendors. All operations on lithium aluminohydride, titanium hydride and titanium tetrachloride were carried out in a helium atmosphere in a glove box. Ball-milling of various quantities of materials, usually 0.5–1.0 g, was performed using 21 g of steel balls in a Spex mill in a hardened-steel vial sealed under helium. Forced air-cooling of the vial was employed to prevent its heating during ball-milling experiments. The majority of hydrogen formed during solid-state transformations promoted by mechanochemical processing of $LiAlH_4$ in the presence of different catalysts remained inside the vial and was detected during its opening. However, it is feasible that some hydrogen gas escaped the vial during the processing and/or was absorbed by the vial walls, and therefore no measurements of the quantities of hydrogen built-up inside the vial during the processing were carried out.

Intermetallic alloys with Al_3Ti, $Al_{22}Fe_3Ti_8$ and Al_3Fe stoichiometries, approximately 10 g each, were prepared by arc-melting mixtures of pure metals in an argon atmosphere on a water-cooled copper hearth. To ensure alloy homogeneity, samples were turned over eight times during arc-melting. Since weight losses during the preparation of alloys did not exceed 0.8 wt.%, the compositions of the alloys were assumed unchanged.

The X-ray powder diffraction (XRD) characterization of the obtained materials was carried out on a Scintag powder diffractometer using Cu Kα radiation. A full profile Rietveld analysis of the powder diffraction data, which were collected at room temperature with a 0.02° 2Θ step, was employed for crystal structure refinement. To protect air-sensitive hydride samples from the atmospheric oxygen and moisture during X-ray powder diffraction experiments, the sample holder containing a hydride powder was covered with an X-ray-transparent polymer film in a glove box under helium.

^{27}Al nuclear magnetic resonance (NMR) experiments were performed on a Chemagnetics Infinity spectrometer operated at 9.4 T (104.2 MHz). Following the preparation, the samples were transferred to the 3.2-mm magic angle spinning (MAS) rotors within a glove box in a helium atmosphere. The ^{27}Al NMR spectra were acquired in a Chemagnetics MAS probe using single-pulse excitation and a spinning rate of 20 kHz. A two-pulse phase modulation (TPPM) decoupling scheme was used to eliminate the line broadening due to the heteronuclear dipolar interaction with ^1H nuclei [14]. The ^{27}Al spectra reported in this work use the δ scale, with positive values downfield, and are referenced with an aqueous solution of aluminum nitrate.

Differential thermal analysis (DTA) of the powder samples was carried out on a Perkin-Elmer DTA 7 unit between 20 and 300°C with a heating rate of 10°C/min in an argon atmosphere. Aluminum oxide crucibles were used as holders and aluminum oxide was used as a reference material. Chemical analysis of selected samples was performed using an ICP-AES technique on a Thermo Jerrell Ash IRIS spectrometer according to a standard ICP-AES procedure [15].

3. Results and discussion

Unlike complex boron- [16] and magnesium-based hydrides [17], little is known about mechanically induced solid-state transformations of complex derivatives of aluminum hydride. Except for a few reports on mechanically induced solid-state reduction of several transition metal halogenides by alkali metal aluminohydrides [18,19] and on mechanochemical preparation of complex aluminohydrides of Li, Na, Mg and Sr [5,9,20–23], no systematic data about mechanochemical behavior of this class of materials is available in the literature.

As we reported in our earlier communication [8], ball-milling of material consisting of 97 mol% of $LiAlH_4$ and 3 mol% of $TiCl_4$ for 5 min at room temperature causes complete transformation of $LiAlH_4$ into Li_3AlH_6, Al and H_2. Only Bragg peaks corresponding to the microcrystalline Li_3AlH_6, Al and LiCl can be seen in the X-ray powder diffraction pattern of the ball-milled hydride (Fig. 1). The differential thermal and gas-volumetric analyses of the mixture (i.e. only one thermal event associated with the decomposition of Li_3AlH_6 was observed, and the amount of hydrogen released during heating to 650°C corresponds to the amount of produced Li_3AlH_6) confirmed the results of X-ray powder diffraction indicating that the transformation proceeds according to Eq. (1), and showed that no other nano-crystalline or amorphous hydride phases undetectable by X-ray powder diffraction formed during the mechanochemical processing (see Ref. [8] for more details):

$$2.91LiAlH_4 + 0.09TiCl_4 = 0.85Li_3AlH_6 + 0.36LiCl + 2.06Al + 0.09[Ti] + 3.27H_2 \quad (1)$$

We also found that $LiAlH_4$ is stable during the mech-

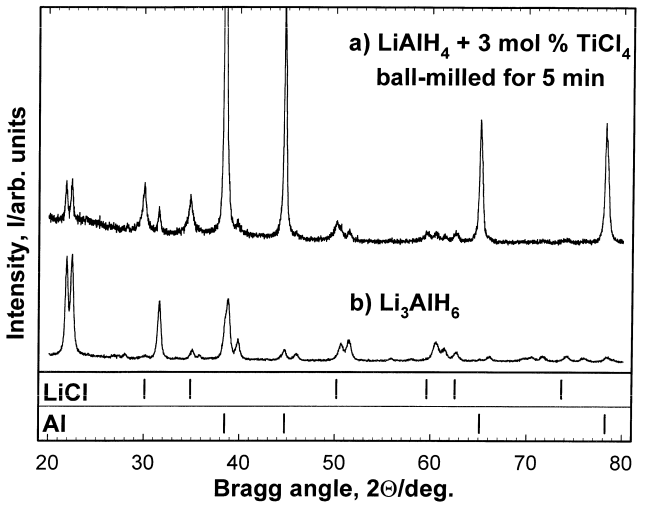

Fig. 1. X-ray powder diffraction patterns of $LiAlH_4$ ball-milled in the presence of 3 mol% $TiCl_4$ for 5 min (a) and Li_3AlH_6 prepared mechanochemically (b). Vertical bars at the bottom of the plot indicate calculated positions of Bragg peaks in LiCl and Al.

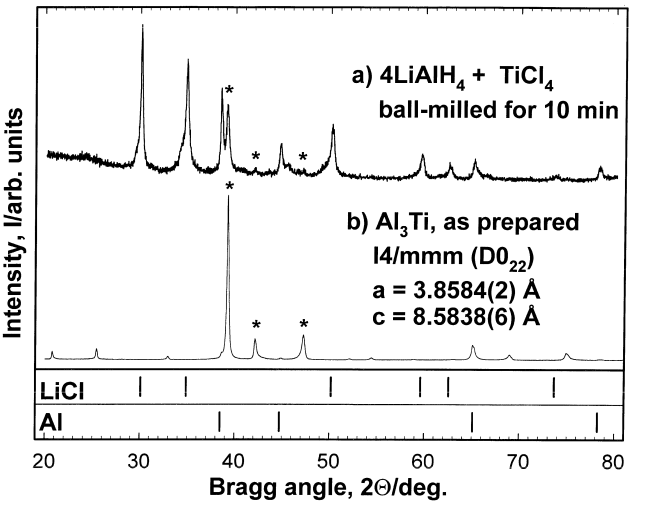

Fig. 2. X-ray powder diffraction patterns of the powder formed after ball-milling of four equivalents of $LiAlH_4$ with one equivalent of $TiCl_4$ for 10 min (a) and the conventionally prepared Al_3Ti (b). Vertical bars at the bottom of the plot indicate calculated positions of Bragg peaks in LiCl and Al. Asterisks indicate the strongest Bragg peaks of the tetragonal Al_3Ti found in both diffraction patterns.

anochemical treatment without a catalyst for up to 35 h [9]. Therefore, the transformations occurring in the $TiCl_4$-doped $LiAlH_4$ during short-term ball-milling were attributed to the presence of an unknown catalytically active titanium species formed from titanium tetrachloride and lithium aluminohydride. Our earlier study [8] also revealed that mechanical treatment is required for these transformations to occur.

To understand the catalytic effect of $TiCl_4$ and to explore the nature of Ti species that catalyze the mechanochemical transformations of $LiAlH_4$, we performed a detailed study of the mechanically activated reaction between stoichiometric amounts of $LiAlH_4$ and $TiCl_4$ (4:1 ratio) as well as the processes occurring in $LiAlH_4$ in the presence of titanium hydride (TiH_2). Due to the high reactivity of the starting materials, we anticipated that TiH_2 might have formed as a product of the mechanochemically promoted reduction of $TiCl_4$ by $LiAlH_4$ and further acted as a catalyst of the mechanochemical transformations of $LiAlH_4$. If this assumption were true, the following reactions would be most likely to describe the mechanism of the observed solid-state rearrangement:

$$TiCl_4 + 4LiAlH_4 = [TiH_2] + 4LiCl + 4Al + 7H_2 \quad (2)$$

$$[TiH_2] + LiAlH_4 = [LiTiAlH_6] \quad (3)$$

$$[LiTiAlH_6] + 2LiAlH_4 = Li_3AlH_6 + [TiH_2] + Al + 3H_2 \quad (4)$$

However, the experimental data do not support this hypothesis. X-ray powder diffraction analysis of the sample obtained after ball-milling of *stoichiometric* amounts (4:1 ratio) of $LiAlH_4$ and $TiCl_4$ for 10 min did not reveal the presence of TiH_2. Only Bragg peaks corresponding to microcrystalline lithium chloride, aluminum and a Ti–Al phase are found in the XRD pattern of the ball-milled material (Fig. 2). Furthermore, gas-volumetric analysis showed no detectable hydrogen gas evolution from the ball-milled sample during heating in vacuum up to 650°C, indicating the absence of any metal hydride phase(s) in the investigated material. The experiments on ball-milling of $LiAlH_4$ with TiH_2 also did not support the mechanism described by Eqs. (2)–(4). Finally, mechanical alloying of $LiAlH_4$–TiH_2 mixtures containing between 3 and 50 mol% TiH_2 for 10 min to 6.5 h did not result in the formation of detectable amounts of Li_3AlH_6.

Another possible explanation of the catalytic effect of $TiCl_4$ on the mechanochemical transformations in $LiAlH_4$ is the formation of a micro/nano-crystalline Al_3Ti intermetallic phase from $TiCl_4$ and $LiAlH_4$, which acts as a dehydrogenation catalyst. The formation of Li_3AlH_6 from $LiAlH_4$ in the presence of $TiCl_4$ could then be described by a sequence of mechanically promoted solid-state mechanochemical reactions as shown by Eqs. (5)–(8). According to the phase diagram of the Ti–Al system [24], Al_3Ti is the richest in aluminum intermetallic phase and, therefore, its formation in the presence of an excess of aluminum (Eq. (6)) is feasible. Since Li_3AlH_6 easily forms during mechanochemical processing of LiH and $LiAlH_4$ [9], it is likely that the transformation of $LiAlH_4$ into Li_3AlH_6 proceeds through the intermediate formation of LiH as a product of the dehydrogenation of $LiAlH_4$ (Eq. (7a)), and a subsequent mechanochemical reaction between LiH and the remaining $LiAlH_4$ (Eq. (7b)). On the other hand, Li_3AlH_6 may also form as a result of the direct solid-state rearrangement of the tetrahedral $[AlH_4]^-$ into the octahedral $[AlH_6]^{3-}$ as shown by Eq. (8). Therefore,

complete understanding of this catalytic solid-state transformation process requires further detailed studies before it is completely understood:

$$TiCl_4 + 4LiAlH_4 = Ti + 4LiCl + 4Al + 8H_2 \quad (5)$$

$$Ti + 4Al = Al_3Ti + Al \quad (6)$$

$$LiAlH_4 \xrightarrow{Al_3Ti\ catalyst} LiH + Al + 1.5H_2 \quad (7a)$$

$$2LiH + LiAlH_4 = Li_3AlH_6 \quad (7b)$$

$$3LiAlH_4 \xrightarrow{Al_3Ti\ catalyst} Li_3AlH_6 + 2Al + 3H_2 \quad (8)$$

The most intense Bragg peak in the X-ray powder diffraction pattern of the sample obtained after ball-milling of $TiCl_4$ with four equivalents of $LiAlH_4$, which could not be assigned to either LiCl or Al, is located at $2\Theta = 39.18°$ (see Fig. 2). According to the literature [25–27], the Al_3Ti intermetallic phase may crystallize in two polymorphic modifications: tetragonal ($D0_{22}$) or cubic ($L1_2$). It is also well known [27] that the metastable Al_3Ti alloy with the cubic $L1_2$-type crystal structure can be prepared by mechanical alloying of Ti and Al powders. Furthermore, Al_3Ti does not react with Al even during prolonged ball-milling [28]. Regardless of which polymorph of Al_3Ti is considered, the strongest Bragg peaks of both the tetragonal $D0_{22}$ (Fig. 2) and cubic $L1_2$ (Fig. 3) phases are located at $2\Theta = 39.2°$, i.e. at the same Bragg angle as the peak in the X-ray powder diffraction pattern of the ball-milled $LiAlH_4$–$TiCl_4$ mixture mentioned above. Unfortunately, the low intensities of the other peaks, which could belong to $D0_{22}$- or $L1_2$-type Al_3Ti, do not provide the definite inference of the crystal structure of this intermetallic phase.

To verify that Al_3Ti intermetallic compound acts as a catalyst of mechanochemical transformations in $LiAlH_4$, we prepared the Al_3Ti ($D0_{22}$) alloy by arc-melting of pure Ti and Al metals, taken in 1:3 atomic ratio, and investigated its influence on mechanically induced transformations of $LiAlH_4$. We also studied the phase transformations of the arc-melted Al_3Ti alloy during high-energy ball-milling and confirmed its transformation into the cubic $L1_2$-type metastable material.

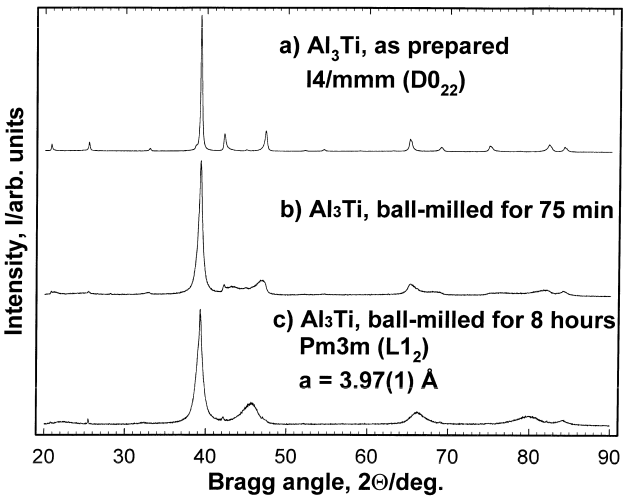

Fig. 3. X-ray powder diffraction patterns of the conventionally prepared Al_3Ti alloy (a) and the materials formed during its ball-milling for 75 min (b) and 8 h (c).

The X-ray powder diffraction pattern of the arc-melted Al_3Ti alloy with the tetragonal ($D0_{22}$) crystal structure and lattice parameters which are in a good agreement with those published previously {$a = 3.8537(8)$, $c = 8.5839(13)$ [25]} is shown in Fig. 2. This alloy gradually transforms into a metastable cubic ($L1_2$) phase during high-energy ball-milling (Fig. 3). Although the phase transformation is close to completion after 8 h of ball-milling, the Bragg peaks corresponding to the tetragonal $D0_{22}$ phase are still visible in the X-ray powder diffraction pattern of the mechanically treated Al_3Ti alloy. Chemical analysis of the obtained powder revealed only minor contamination of the sample with the vial material (Fe). The iron content of Al_3Ti ball-milled for 8 h was found to be only 1.72% by weight or 0.98 at% Fe. However, since iron is well known as an alloying element capable of stabilizing metastable phases in the Al_3Ti system [29], its introduction into the sample during mechanical alloying could also be responsible for the observed transformation of the $D0_{22}$ phase into the metastable $L1_2$ phase.

The catalytic effect of Al_3Ti on the phase transformations in $LiAlH_4$ was investigated under conditions similar to those used in the experiments with $TiCl_4$. A mixture containing 97 mol% $LiAlH_4$ and 3 mol% bulk polycrystalline Al_3Ti with the $D0_{22}$-type crystal structure was ball-milled for 10 min, 75 min, and 7.5 h in a Spex mill under helium. The obtained hydride powders were investigated using X-ray powder diffraction, solid-state ^{27}Al NMR and differential thermal analysis.

Analysis of the Al_3Ti-doped hydride powders formed during mechanochemical treatment for 10 and 75 min reveals only minor changes in their phase composition. Considering the fact that Al_3Ti was added in bulk form, it is not surprising that its interaction with $LiAlH_4$ was slow until the alloy was crushed into a fine powder. However, ball-milling for 7.5 h has a considerable effect on the hydride material. Both X-ray powder diffraction and ^{27}Al NMR spectroscopy unambiguously confirm the catalytic properties of Al_3Ti. The X-ray powder diffraction pattern of $LiAlH_4$ ball-milled for 7.5 h in the presence of 3 mol% Al_3Ti and the diffraction patterns of the starting $LiAlH_4$ and the mechanochemically prepared Li_3AlH_6 [9] are shown in Fig. 4. The peaks representing Li_3AlH_6 and the residual $LiAlH_4$ species along with the strong peaks of microcrystalline aluminum are clearly distinguishable in this pattern.

The above results are consistent with the spectra obtained using solid-state ^{27}Al NMR spectroscopy. The ^{27}Al

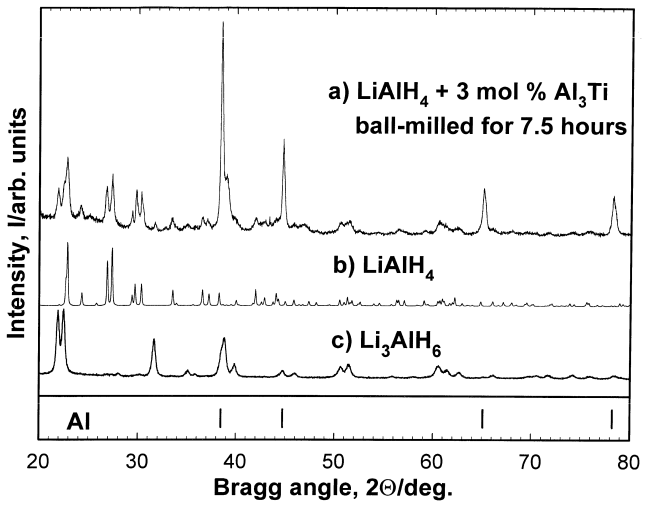

Fig. 4. X-ray powder diffraction patterns of $LiAlH_4$ ball-milled in the presence of 3 mol% Al_3Ti for 7.5 h (a), the starting $LiAlH_4$ (b) and Li_3AlH_6 prepared mechanochemically (c). Vertical bars at the bottom of the plot indicate calculated positions of Bragg peaks in Al.

MAS spectrum of $LiAlH_4$ doped with 3 mol% Al_3Ti and ball-milled for 7.5 h contains three resonance signals at around -34, 104 and 1640 ppm (see Fig. 5a), which represent Li_3AlH_6, $LiAlH_4$ and metallic aluminum, respectively. These assignments are based on our previous solid-state NMR investigations of $LiAlH_4$ and Li_3AlH_6, which revealed that the shifts of ^{27}Al in these materials are 103.8 (± 0.8) ppm and -33.7 (± 0.8) ppm, respectively (see Fig. 5b,c) [30]. The large shift of the resonance at around 1640 ppm is attributed to the so-called Knight shift interaction in metallic aluminum [31]. Since none of these resonances could be assigned to Al_3Ti, we also acquired two supplementary ^{27}Al MAS NMR spectra of pure Al_3Ti alloy before and after ball-milling for 8 h. In its original state

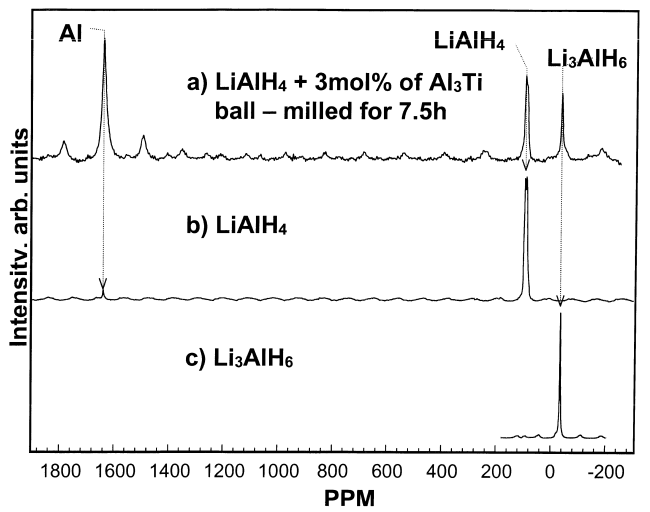

Fig. 5. ^{27}Al MAS NMR spectra of $LiAlH_4$ ball-milled in the presence of 3 mol% Al_3Ti for 7.5 h (a), the starting commercial $LiAlH_4$ containing trace amounts of Al (b) and Li_3AlH_6 prepared mechanochemically [9] (c). Isotropic NMR resonances are marked by arrows.

Al_3Ti has the tetragonal crystal structure, whereas the mechanical treatment produces a nearly amorphous cubic phase. However, only the crystalline form of Al_3Ti has been observed as a narrow resonance at 2645 ppm with full width at half magnitude (FWHM) of 2.3 kHz (spectrum not shown). The resonance signal in the ^{27}Al spectrum of the ball-milled sample was too broad to be observed under the conditions used in our experiment.

We note that the spectra in Fig. 5 are not completely quantitative due to several complicating factors. First, the resonances at 104 and -34 ppm represent only the so-called central ($m = +1/2 \leftrightarrow m = -1/2$) transition of ^{27}Al nuclei, which corresponds to 9/35 of the total intensity for these sites [32]. Due to the considerable quadrupolar broadening, the satellite transitions for these sites are observed as wide manifolds of spinning sidebands. In contrast, metallic aluminum has a cubic structure, which leads to degeneracy of all the transitions [31]. Thus, the entire intensity of the metal peak is accounted for in the resonance at 1640 ppm and a couple of associated spinning sidebands (which are best observable in Fig. 5a). Second, the rf excitation and the probe tuning were optimized for the central transition of $LiAlH_4$, which had the opposite effect of reducing the intensity of the peak at 1640 ppm. Therefore, we calibrated the spectral intensities in Fig. 5 using the same experimental conditions to acquire a ^{27}Al MAS NMR spectrum of a known 1:1:1 molar mixture of $LiAlH_4$, Li_3AlH_6, and Al. The results showed that 50(± 5)% of $LiAlH_4$ in the ball-milled sample was transformed into Li_3AlH_6 and Al.

Differential thermal analysis also reveals significant changes in the thermochemical behavior of the hydride doped with Al_3Ti and ball-milled for 7.5 h as compared with the pure $LiAlH_4$. We note that the thermochemical behavior of pure $LiAlH_4$ has been studied extensively (e.g. see Refs. [9,33–35]), and it is well known that the thermal decomposition of $LiAlH_4$ into Li_3AlH_6, H_2 and Al is exothermic, while the decomposition of Li_3AlH_6 into LiH, Al and H_2 is endothermic. As shown in Fig. 6, the number of thermal events in the DTA trace of the Al_3Ti-doped and ball-milled material between room temperature and 300°C is reduced to only two — an exothermic effect between 122 and 150°C, with a maximum at 132°C, and an endothermic effect between 178 and 242°C, with a minimum at 207°C. Furthermore, the exothermic event (122–150°C, minimum at 132°C), which most certainly corresponds to the decomposition of $LiAlH_4$ remaining in the Al_3Ti-doped sample after ball-milling, occurs at ~50°C lower temperatures when compared with that observed in pure lithium aluminohydride (178–220°C, maximum at 188°C) [9]. The endothermic effect seen in pure $LiAlH_4$ (160–178°C, minimum at 170°C) due to melting of $LiAlH_4$ [9] disappears from the DTA trace of the Al_3Ti-doped and ball-milled $LiAlH_4$. Simultaneously, the intensity of the endothermic event (185–240°C, minimum at 207°C) accompanying the decomposition of Li_3AlH_6

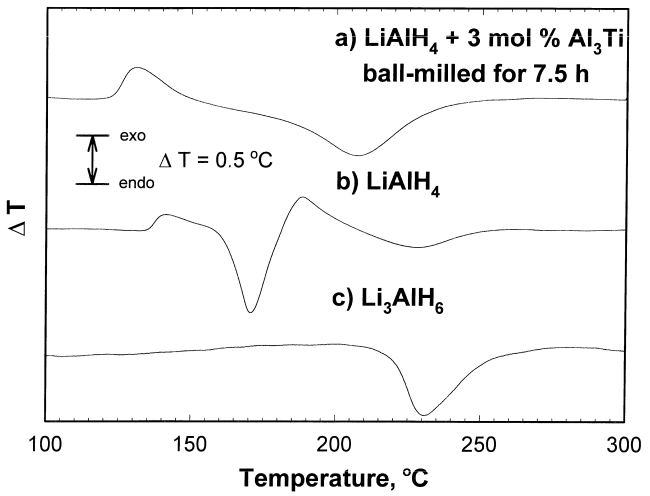

Fig. 6. DTA traces of $LiAlH_4$ ball-milled in the presence of 3 mol% Al_3Ti for 7.5 h (a), the starting $LiAlH_4$ (b), and Li_3AlH_6 prepared mechanochemically (c).

significantly increases in the Al_3Ti-containing and processed material. The position of this event is also shifted by ~20°C towards lower temperatures compared to pure $LiAlH_4$ [9]. Since our previous investigations of the mechanochemical stability of $LiAlH_4$ [9] revealed fairly high stability of this aluminohydride during prolonged ball-milling without catalysts, the mechanochemical transformations observed in $LiAlH_4$ in the presence of the Al_3Ti alloy are attributed to the catalytic effect of the Al_3Ti intermetallic compound. We also note that Ti-based catalysts have a similar effect on the thermal decomposition of sodium aluminohydride; see Refs. [2–7] for more details.

The obtained results offer a plausible explanation of the catalytic behavior of $TiCl_4$ during the mechanochemical transformation of $LiAlH_4$ into Li_3AlH_6, Al and H_2 [8]. It appears that $TiCl_4$ is rapidly reduced by $LiAlH_4$ giving rise to nano/microcrystalline Ti and Al, which further react with the formation of a Al_3Ti intermetallic phase (Eqs. (5) and (6)). The latter then acts as a heterogeneous dehydrogenation catalyst enabling the mechanochemical transformation according to Eqs. (7a,b) or Eq. (8). It is also quite obvious that the activity of an in situ prepared nano/microcrystalline heterogeneous metal catalyst with an extremely large active surface area significantly exceeds that of a bulk metal [36], which explains the higher catalytic activity of $TiCl_4$ in comparison to the Al_3Ti alloy.

Since the phase transformation in the Al_3Ti alloy during high-energy ball-milling for 8 h raises the possibility that iron impurities stabilize the $L1_2$-type Al_3Ti, which in turn may be responsible for the catalytic properties of the Al_3Ti alloy, we prepared a polycrystalline $L1_2$-type material with the chemical composition $Al_{22}Fe_3Ti_8$, and tested its catalytic activity. We also prepared an iron–aluminum alloy with the chemical composition Al_3Fe and investigated its effect on the behavior of $LiAlH_4$ during high-energy ball-milling. Both Al_3Fe and $Al_{22}Fe_3Ti_8$ were prepared by arc-melting stoichiometric amounts of the pure metals and were found to be essentially single phase materials. The lattice parameters of both materials agree well with those published previously {$Al_{22}Fe_3Ti_8$, this work, space group *Pm3m*, $a = 3.94(1)$; Ref. [26], space group *Pm3m*, $a = 3.93$ Å. Al_3Fe, this work, space group *C2/m*, $a = 15.5242(6)$ Å, $b = 8.0474(4)$ Å, $c = 12.4612(5)$ Å, $\beta = 107.717(2)°$; Ref. [37], space group *C2/m*, $a = 15.509(3)$ Å, $b = 8.066(2)$ Å, $c = 12.469(2)$ Å, $\beta = 107.72(2)°$}.

Our experiments on mechanical alloying of $LiAlH_4$ with 3 mol% of $Al_{22}Fe_3Ti_8$ alloy show that the catalytic activity of this material is considerably lower than that observed for Al_3Ti. According to the ^{27}Al NMR data of Fig. 7 (after calibrating the intensities as described above) only about 16 and 10% of $LiAlH_4$ has reacted when the hydride was doped with $Al_{22}Fe_3Ti_8$ and Al_3Fe, respectively. We note, however, that the catalytic activity of Al_3Fe is considerably higher than that of pure iron observed in our previous experiments [9].

Because of the complex nature of chemical and phase transformations, which occur simultaneously in $LiAlH_4$ and Al_3Ti during mechanochemical processing, it is rather difficult to conclude whether and how the crystal structure of the Al_3Ti alloy influences its properties as a catalyst. So far, we have found no direct evidence supporting the possibility that the catalytic behavior of Al_3Ti alloy is dependent on its crystal structure. A substantial decrease in the ability of the Al–Ti–Fe system to promote mechanochemical transformations in $LiAlH_4$ with increasing iron content is, however, in line with previously reported data on the behavior of metallic alloys as heterogeneous catalysts [36]. It is well known that dilution of an active metal (i.e. Ti) with an inactive one causes significant reduction of the hydriding–dehydriding activity of the

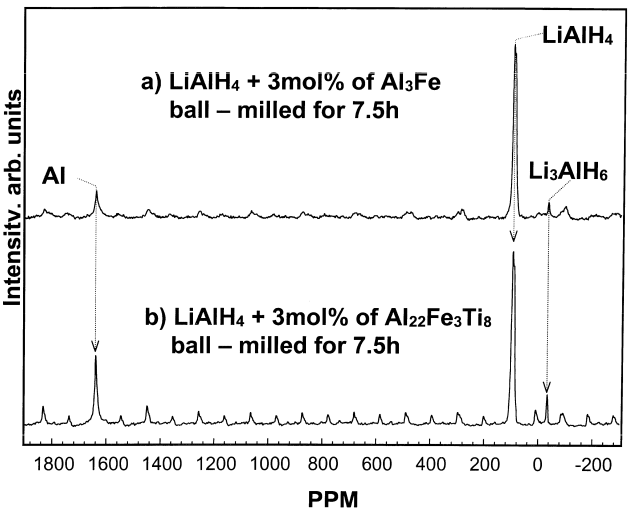

Fig. 7. ^{27}Al MAS NMR spectra of $LiAlH_4$ ball-milled in the presence of 3 mol% Al_3Fe (a) and 3 mol% $Al_{22}Fe_3Ti_8$ (b) for 7.5 h. Isotropic resonances are marked by arrows.

metallic alloy in comparison to that of the pure active metal.

4. Conclusions

Our investigations of the ability of Ti- and Fe-based catalysts to promote the mechanochemical transformation of lithium aluminum hydride into lithium hexahydroaluminate, aluminum and hydrogen revealed that the activity of the tested catalysts gradually decreases from $TiCl_4$ to Fe in the series $TiCl_4 > Al_3Ti \gg Al_{22}Fe_3Ti_8 > Al_3Fe > Fe$. The high catalytic activity of $TiCl_4$ in the mechanically induced transformation of $LiAlH_4$ is attributed to the in situ formation of a nano/microcrystalline Al_3Ti phase from $TiCl_4$ and $LiAlH_4$ during ball-milling. The high catalytic activity of the Al_3Ti formed in situ is in line with the expectation that an extremely large $Al_3Ti/LiAlH_4$ interface area is achieved during mechanical alloying of $LiAlH_4$ with a catalytic amount of $TiCl_4$.

Acknowledgements

The Ames Laboratory is operated for the U.S. Department of Energy (DOE) by Iowa State University under contract No.W-7405-ENG-82. Different aspects of this work were supported by the Office of Basic Energy Sciences, Materials Sciences Division (VBB, KWD, and VKP) and the Chemical Sciences Division (JWW and MP) of the U.S. DOE, and by Iowa State University Roy J. Carver Trust Grant (VPB and VKP).

References

[1] G. Sandrock, in: Y. Yürüm (Ed.), Hydrogen Energy Systems, Kluwer Academic, Dordrecht, 1995, p. 135.
[2] B. Bogdanovic, M.J. Schwickardi, J. Alloys Comp. 253 (1997) 1.
[3] R.A. Zidan, S. Takara, A.G. Hee, C.M. Jensen, J. Alloys Comp. 285 (1999) 119.
[4] C.M. Jensen, R.A. Zidan, N. Mariels, A.G. Hee, C. Hagen, Int. J. Hydrogen Energy 24 (1999) 461.
[5] L. Zaluski, A. Zaluska, J.O. Ström-Olsen, J. Alloys Comp. 290 (1999) 71.
[6] B. Bogdanovic, R.A. Brand, A. Marjanovic, M. Schwickardi, J. Tölle, J. Alloys Comp. 302 (2000) 36.
[7] K.J. Gross, S. Guthrie, S. Takara, G. Thomas, J. Alloys Comp. 297 (2000) 270.
[8] V.P. Balema, K.W. Dennis, V.K. Pecharsky, Chem. Commun. (Oxford) (2000) 1665.
[9] V.P. Balema, K.W. Dennis, V.K. Pecharsky, J. Alloys Comp. 313 (2000) 69.
[10] V.C.Y. Kong, F.R. Foulkes, D.W. Kirk, J.T. Hinatsu, Int. J. Hydrogen Energy 24 (1999) 665.
[11] F. Lynch, B.J. Mork, J.S. Wilkes, in: Proc. Intersoc. Energy Convers. Eng. Conf. 33, 1998, IECEC217/1–IECEC217/6.
[12] C.A. Ward, Can. Patent 2028978, 1992.
[13] R.W. Breault, J. Rolfe, Proc. Power Sources Conf. 39 (2000) 184.
[14] A.E. Bennett, C.M. Rienstra, M. Auger, K.V. Lakshmi, R.G. Griffin, J. Chem. Phys. 103 (1995) 6951.
[15] S.J. Hill (Ed.), Inductively Coupled Plasma Spectrometry and Its Applications, Sheffield Academic Press, Sheffield, UK, 1999.
[16] V.V. Volkov, K.G. Myakishev, Inorg. Chim. Acta 289 (1999) 51.
[17] I.G. Kostanchuk, E.Yu. Ivanov, V.V. Boldyrev, Russ. Chem. Rev. 67 (1998) 69.
[18] V.V. Volkov, A.I. Golovanova, N.N. Maltseva, K.G. Myakishev, N.T. Kusnetsov, Izv. Sib. Otd. Akad. Nauk SSSR, Ser. Khim. Nauk (1988) 67.
[19] N.N. Maltseva, K.G. Myakishev, A.I. Golovanova, V.V. Volkov, N.T. Kusnetsov, Zh. Neorg. Khim. 34 (1989) 40.
[20] T.N. Dymova, V.N. Konoplev, A.S. Sizareva, D.P. Aleksandrov, Russ. J. Coord. Chem. 25 (1999) 312.
[21] T.N. Dymova, V.N. Konoplev, A.S. Sizareva, D.P. Aleksandrov, N.T. Kuznetsov, Dokl. Akad. Nauk 359 (1998) 200.
[22] T.N. Dymova, D.P. Aleksandrov, V.N. Konoplev, T.A. Silina, N.T. Kuznetsov, Russ. J. Coord. Chem. 19 (1993) 491.
[23] J. Hout, S. Boily, V. Güther, R. Schultz, J. Alloys Comp. 283 (1999) 304.
[24] U.R. Kattner, I.C. Lin, Y.A. Chang, Metall. Trans. A 23 (1992) 2081.
[25] P. Norby, A.N. Christensen, Acta Chem. Scand. 40A (1986) 157.
[26] A. Seibold, Z. Metallkd. 72 (1981) 712.
[27] S. Srinivasan, P.B. Desch, R.B. Schwarz, Scripta Metall. Mater. 25 (1991) 2513.
[28] H. Sugiyama, J. Kaneko, M. Sugamata, Mater. Sci. Forum 88 (1992) 361.
[29] T.Y. Yang, E. Goo, Metal Mater. Trans. 26A (1995) 1029.
[30] V.P. Balema, J.W. Wiench, M. Pruski, V.K. Pecharsky, unpublished.
[31] L. Kellberg, H. Blidsoe, H.J. Jakobsen, J. Chem. Soc., Chem. Commun. (1990) 1294.
[32] D. Freude, J. Haas, in: P. Diehl, E. Fluck, R. Kosfeld (Eds.), NMR Basic Principles and Progress, Vol. 29, Springer, Berlin, 1993, p. 1.
[33] J.A. Dilts, E.C. Ashby, Inorg. Chem. 11 (1972) 1230.
[34] T.N. Dymova, V.N. Konoplev, D.P. Aleksandrov, A.S. Sizareva, T.A. Silina, Russ. J. Coord. Chem. 21 (1995) 165.
[35] J.P. Bastide, B.M. Bonnetot, J.M. Letoffe, P. Claudy, Mater. Res. Bull. 20 (1985) 999.
[36] V. Ponec, G.C. Bond, Catalysis by Metals and Alloys, Elsevier, Amsterdam, 1995.
[37] A. Griger, V. Stefaniay, T. Turmezey, Z. Metallkd. 77 (1986) 30.